Increasing the synchronization stability in complex networks

Wu, Xian; Xi, Kaihua; Cheng, Aijie; Lin, Hai Xiang; van Schuppen, Jan H.

DOI
10.1063/5.0114974

Publication date
2023

Document Version
Final published version

Published in
Chaos (Woodbury, N.Y.)

RESEARCH ARTICLE | APRIL 10 2023

Increasing the synchronization stability in complex networks

Xian Wu; Kaihua Xi ✉; Aijie Cheng; ... et. al

Chaos 33, 043116 (2023)
https://doi.org/10.1063/5.0114974

Increasing the synchronization stability in complex networks

Cite as: Chaos 33, 043116 (2023); doi: 10.1063/5.0114974
Submitted: 26 July 2022 · Accepted: 20 March 2023 ·
Published Online: 10 April 2023

Xian Wu,[1] Kaihua Xi,[1,a)] Aijie Cheng,[1] Hai Xiang Lin,[2] and Jan H. van Schuppen[2]

AFFILIATIONS

[1]School of Mathematics, Shandong University, Jinan, Shandong 250100, China
[2]Delft Institute of Applied Mathematics, Delft University of Technology, Delft 2628 CD, The Netherlands

[a)]**Author to whom correspondence should be addressed:** kxi@sdu.edu.cn

ABSTRACT

We aim to increase the ability of coupled phase oscillators to maintain synchronization when the system is affected by stochastic disturbances. We model the disturbances by Gaussian noise and use the mean first hitting time when the state hits the boundary of a secure domain, that is a subset of the basin of attraction, to measure synchronization stability. Based on the invariant probability distribution of a system of phase oscillators subject to Gaussian disturbances, we propose an optimization method to increase the mean first hitting time and, thus, increase synchronization stability. In this method, a new metric for synchronization stability is defined as the probability of the state being absent from the secure domain, which reflects the impact of all the system parameters and the strength of disturbances. Furthermore, by this new metric, one may identify those edges that may lead to desynchronization with a high risk. A case study shows that the mean first hitting time is dramatically increased after solving corresponding optimization problems, and vulnerable edges are effectively identified. It is also found that optimizing synchronization by maximizing the order parameter or the phase cohesiveness may dramatically increase the value of the metric and decrease the mean first hitting time, thus decrease synchronization stability.

Synchronization of coupled phase oscillators has served as a paradigm for understanding collective behavior of real complex systems, where examples arise in nature (e.g., chimera spatiotemporal patterns,[1] and cardiac pacemaker cells[2]) and artificial systems (e.g., multi-agent systems,[3] distributed optimization,[4] and power grids[5,6]). For systems such as a power grid if synchronization is lost, then the system can no longer function properly. The objective of this paper is to propose a method to increase the ability of these systems to maintain synchronization under disturbances, which is called synchronization stability. We introduce a new metric for the analysis of synchronization stability, which not only reflects the role of system parameters, i.e., the natural frequency, the network topology, and the coupling strength, but also reflects the role of strength of disturbances at nodes. With this metric as the objective of an optimization framework, the synchronization stability can be optimized by redistributing either natural frequencies of nodes and coupling strength of edges. In addition, the vulnerable edges that limit synchronization stability can be effectively identified by this metric. The result of this paper provides a new avenue for the analysis of synchronization stability of complex networks.

I. INTRODUCTION

On synchronization of complex networks, significant insights have been obtained from investigations on the emergence of a synchronous state and synchronization coherence. The synchronization is determined by system parameters, including natural frequencies at nodes, the network topology, and the coupling strength of edges. With the metrics of critical coupling strength[7,8] and the order parameter,[9] the influences of these parameters on synchronization are widely investigated. Based on these investigations, the system parameters may be assigned to optimize the synchrony, which can be attained by deletion or addition of edges or by changing the coupling strength of edges in the network. An important problem is to maintain synchronization when the system is subjected to disturbances. Regarding the ability to maintain synchronization, the spectrum of the system matrix of the linearized system and the volume of the basin of attraction of a stable synchronous state may be investigated.[10–12] However, in these investigations, the severity of disturbances are not considered and the edges at which synchronization may be lost cannot be effectively identified.

In control theory, the synchronous state is also mentioned as the *set point* for control, in which control actions are taken to let

the state converge to the synchronous state after disturbances. Thus, with frequently occurring disturbances, the phase may fluctuate around the synchronous state. If the fluctuations in phase differences are so large that the state of the system cannot stay inside a neighborhood of the synchronous state, then synchronization is lost. We say an edge is more vulnerable if desynchronization occurs at this edge more easily. The $\mathscr{H}_2$ norm of a linear input–output system is often used to study the synchronization performance after disturbances.[13–15] By minimizing this $\mathscr{H}_2$ norm as an objective and system parameters as decision variables, the fluctuations in phase differences may be effectively suppressed. In a framework of the theory of stochastic processes, the dependence (or relationship) between the fluctuation of the phase difference in each edge and the system parameters is revealed, in which the cycle space of graphs plays a role.[16]

However, it is insufficient to focus on the fluctuations in phase differences only for the synchronization stability analysis. In fact, the risk of losing synchronization is actually determined by two factors, i.e., the fluctuations of the state and the size of the basin attraction of the synchronous state. Note that due to the nonlinearity of the system, the fluctuations of the state also depend on the synchronous state.[16] Thus, to increase synchronization stability of a system with disturbances, it is important to find such a synchronous state that has a large basin of attraction and around which the fluctuation of the state is also small. The concept of the first hitting time of a stochastic process, which is a random variable, is often used to study the stability of nonlinear systems.[17,18] For the stability analysis of coupled phase oscillators, the first hitting time can be defined as the first time when the state starting at the synchronous state hits the boundary of the basin of attraction. Clearly, this first hitting time depends on both the size of the basin of attraction of the synchronous state and fluctuations of the state. The larger the mean of this first hitting time, the higher probability of the state staying in the basin of attraction and the stronger ability to maintain synchronization. However, due to the nonlinearity and high dimension of the system, the boundary of the basin of attraction of the synchronous state can hardly be precisely estimated. A sign of losing synchronization is that there are edges in which the absolute values of phase differences become larger than $\pi/2$ and then go to infinity as time increases to infinity. Thus, we focus on the domain in which the absolute values of phase differences in the edges are all smaller than $\pi/2$, which is called *the secure domain* in this paper. Clearly, if phase differences in the edges are in the secure domain for all the time, the system maintains synchronization.[19] Once the state goes out of this secure domain, the synchronization may be lost. Hence, with this secure domain, the concept of the first hitting time can be applied to the complex system.

In this paper, we model frequently occurring disturbances in the nonlinear dynamics by Gaussian noise and investigate the risk of the state going out of the secure domain in the corresponding nonlinear stochastic process. If one linearizes the nonlinear stochastic system, then the resulting linear stochastic system driven by a Brownian motion process has a Gaussian invariant probability distribution. Based on this invariant probability distribution, we define a metric for the risk of the state of the nonlinear stochastic process going out of the secure domain and propose an optimization framework to minimize this metric, thus increase the mean first time when the state starting at the synchronous state hits the boundary of the secure domain. We show the range of this metric, and by the optimization framework, we address the design problem of the coupling strength and the natural frequency, respectively. It will be shown that after maximizing the probability of the states of the Gaussian process inside the secure domain, the mean first hitting time is effectively increased, which indicates an increase in synchronization stability.

This paper is organized as follows. The model of coupled phase oscillators is introduced in Sec. II. We describe the concept of the mean first hitting time and the invariant probability distribution of the linear stochastic process in Secs. III and IV and propose an optimization method to decrease the risk of the state being absent from the secure domain in Sec. V. A case study for the evaluation of the performance of the optimization framework is presented in Sec. VI. We conclude this paper with perspectives in Sec. VII.

II. THE MODEL

We consider an undirected graph $\mathscr{G} = (\mathscr{V}, \mathscr{E})$ with n nodes in the set $\mathscr{V}$ and m edges in the set $\mathscr{E}$. The dynamics of coupled phase oscillators are described by the following differential equation:

$$\dot{\varphi}_i(t) = \omega_i - \sum_{j=1}^{n} l_{ij} \sin(\varphi_i(t) - \varphi_j(t)), \text{ for } \quad i = 1, 2, \ldots, n, \tag{1}$$

where φ_i is the phase of oscillator i, ω_i represents the natural frequency, l_{ij} denotes the coupling strength of the edge $(i,j) \in \mathscr{E}$ that connects nodes i and j, and $l_{ij} > 0$ if nodes i and j are connected and $l_{ij} = 0$ otherwise. It is assumed that the graph is connected, thus it holds $m \geq n - 1$.

Without loss of generality, we assume that $\sum_{i=1}^{n} \omega_i = 0$, and there exists a synchronous state $\boldsymbol{\varphi}^* = \mathrm{col}(\varphi_i^*) \in \mathbb{R}^n$ such that

$$\omega_i - \sum_{j=1}^{n} l_{ij} \sin(\varphi_i^* - \varphi_j^*) = 0, \quad i = 1, 2, \ldots, n, \tag{2}$$

which can be typically obtained by increasing the coupling strength of the edges. We focus on the synchronous state in the following domain:

$$\Theta = \{\boldsymbol{\varphi} \in \mathbb{R}^n \big| |\varphi_i - \varphi_j| < \pi/2, \forall (i,j) \in \mathcal{E}\}, \tag{3}$$

which in this paper is called *the secure domain* for the stability analysis. It has been shown that the synchronous state in this domain is asymptotically stable and by the Lyapunov method for stability analysis, the state of system (1) starting inside this domain will converge to a synchronous state in this domain.[19] If synchronization is lost, the state of the system must have gone out of this secure domain. Conversely, if the state of the system stays in this domain at any time, synchronization is maintained. Thus, to increase synchronization stability, it is critical to decrease the risk that the state leaving this secure domain.

Due to disturbances brought to the natural frequency, the system may lose its synchronization. The application of perturbation is an effective way to study fluctuations of the state caused by

disturbances, in which the focus is the dynamics,

$$\dot{\varphi}_i(t) = \omega_i - \sum_{j=1}^{n} l_{ij} \sin(\varphi_i(t) - \varphi_j(t)) + \Delta\omega_i(t), \ i = 1, \ldots, n, \quad (4)$$

where $\Delta\omega_i(t)$ denotes the frequently occurring disturbance at node i. In this paper, the theory of the stochastic process is used to study synchronization stability. We model the disturbance $\Delta\omega_i$ by Gaussian noise and focus on the following stochastic process:

$$\dot{\varphi}_i(t) = \omega_i - \sum_{j=1}^{n} l_{ij} \sin(\varphi_i(t) - \varphi_j(t)) + b_i w_i(t), \text{ for } i = 1, \ldots, n, \quad (5)$$

where the variable $w_i(t)$ represents a standard Gaussian white noise process affecting node i. For any two distinct nodes i and j, the stochastic processes w_i and w_j are assumed to be independent. The variable b_i specifies the standard deviation of the noise. It is remarked that Eq. (4) describes a deterministic system while Eq. (5) describes a stochastic system. The latter system models detail the fluctuations of the state of the system due to disturbances and, hence, is more suitable to investigate synchronization stability in case of such disturbances. In addition, the disturbance in (4) may be bounded while the one modeled by Gaussian noise in (5) is unbounded.

When the system loses its synchronization, there is at least one edge in which the absolute value of the phase differences goes to infinity as time increases to infinity. We denote $e_k = (i, j) \in \mathscr{E}$ for $k = 1, \ldots, m$. To obtain information about the phase differences of all the edges in the network, we define the output of the system (5) as those phase difference according to the formula,

$$y_k(t) = \varphi_i(t) - \varphi_j(t), \text{ for } k = 1, \ldots, m, \quad (6)$$

where k is the index of edge $e_k = (i, j)$ in the edge set $\mathscr{E}$. Here, the direction of edge e_k is from node i to j, which is required to obtain phase differences in the output. This direction is arbitrarily specified, which has no impact on the following analysis. In the remainder of this paper, the vector notations $\boldsymbol{\varphi}(t) = \mathrm{col}(\varphi_i(t)) \in \mathbb{R}^n$ for the state variables in (5) and $\boldsymbol{y}(t) = \mathrm{col}(y_k(t)) \in \mathbb{R}^m$ for the output in (6) will be used for simplicity. Corresponding to phase $\boldsymbol{\varphi}^*$ at the synchronous state, the output is denoted by

$$\boldsymbol{y}^* = \mathrm{col}(y_k^*) \in \mathbb{R}^m \text{ with } y_k^* = \varphi_i^* - \varphi_j^*. \quad (7)$$

For the deterministic system (1), with the metrics of *the order parameter*, or *the critical coupling strength*, or *the phase cohesiveness* that is the $\mathscr{L}_\infty$ norm of $\boldsymbol{y}^*$, the synchronization may be improved by designing the network topology and redistributing the natural frequencies. See Appendix A for the definition of the order parameter. Here, the critical coupling strength is defined as the smallest coupling strength of the edges at which a phase transition from incoherency to synchronization occurs.[20]

III. THE MEAN FIRST HITTING TIME

The first hitting time model is often used to study the survival time of a system,[18] which is also used to study the stability of nonlinear systems.[17] In a first hitting time model, there are two components, i.e., a stochastic process $\{\boldsymbol{x}(t) \in \mathbb{X}, t \in \mathbb{T}\}$ with initial value $\boldsymbol{x}(0) = \boldsymbol{x}_0$, where $\mathbb{X}$ is the state space of the process, a boundary set $\mathbb{B} \subset \mathbb{X}$ and $\mathbb{T} = [0, +\infty)$. Assume that the initial value of the process x_0 lies outside of the boundary set $\mathbb{B}$, then the first hitting time can be defined by the random variable $t_e : \Omega \to \mathbb{T}$,

$$t_e = \begin{cases} \inf_{t \in \mathbb{T}} x(t) \in \mathbb{B}, & \text{if such a } t \in \mathbb{R}_+ \text{ exists}, \\ +\infty, & \text{else}, \end{cases} \quad (8)$$

where t_e is the first time when the sample path of the stochastic process reaches the boundary set $\mathbb{B}$. The first hitting time is also called *the first exit time* when the sample path of the stochastic process exits a set $\mathbb{A}$ with $\partial\mathbb{A} = \mathbb{B}$ and the initial state lying inside $\mathbb{A}$. Clearly, this first hitting time depends on the probability distribution function of the stochastic process $\boldsymbol{x}(t)$, the initial value, and the boundary set $\mathbb{B}$. For some specific stochastic processes, such as the Wiener process and the Ornstein–Uhlenbeck process, the probability density of the first hitting time can be analytically derived.[21,22] For a complex stochastic process such as the one described by (5), the moment of the first hitting time can be approximated by the Monte Carlo method, i.e., given an initial value and a boundary set, the distribution of the first hitting time can be approximated by simulating the stochastic process, and then the moment can be computed with a large amount of simulations.

For the system (5), to use the first hitting time model, the boundary set can be $\mathbb{B} = \partial\mathbb{A}$, where the set $\mathbb{A}$ denotes the basin of the attraction and the state space $\mathbb{X} = \mathbb{R}^n$. Clearly, similar as synchronization stability, the expectation of the first hitting time depends on the size of the basin of attraction and the severity of disturbances. Thus, the expectation of the first time when the state hits the boundary of the basin of the attraction can be used to characterize the synchronization stability. However, due to the difficulty in estimating the boundary of the basin of attraction, the expectation of the first exit time is difficult to be precisely estimated even by statistics of simulations based on the Monte Carlo method. Alternatively, the first exit time of the state from the secure domain Θ, rather than from the basin of attraction, is used to characterize the synchronization stability. Correspondingly, in the first hitting time model, one chooses the boundary of the secure domain according to $\mathbb{B} = \partial\Theta$ and $\mathbb{A} = \Theta$. A larger first hitting time implies a longer period of synchronization stability and an increased stability against disturbances. Because this secure domain is a subset of the basin of attractions of the synchronous state, this first hitting time is smaller than the survival time of the system.

The distribution of the first hitting time is closely related to the probability density function of the state of system (5). The probability density of the system (5) can be solved from the corresponding *Forward Kolmogorov Equation*,[17] which, however, is very complex because of the high dimension of the system. Thus, we do not aim to derive the analytical form of the probability density function of the first hitting time but focus on its mean $\bar{t}_e$ which is computed approximately by the Monte Carlo method in which a large amount of simulations of (5) with initial state $\boldsymbol{x}_0$ at the synchronous state are performed. These simulations will be carried out in the section of case study to show the changes in synchronization stability. This is practical because stochastic disturbances, which may be independent on the state, occur continuously even when the state is at the synchronous state.

IV. THE INVARIANT PROBABILITY DISTRIBUTION OF A LINEAR STOCHASTIC PROCESS

Now, we focus on the following linear stochastic system:

$$\begin{aligned}\dot{\widehat{\boldsymbol{\varphi}}}(t) &= -\boldsymbol{L}_a\widehat{\boldsymbol{\varphi}}(t) + \boldsymbol{B}\boldsymbol{w}(t),\\ \widehat{\boldsymbol{y}}(t) &= \boldsymbol{C}^\top\widehat{\boldsymbol{\varphi}}(t),\end{aligned} \tag{9}$$

which is linearized from (5) at the synchronous state $\boldsymbol{\varphi}^*$. Here, the state variable $\widehat{\boldsymbol{\varphi}}$ and the output $\widehat{\boldsymbol{y}}(t)$ represent the deviation of the state $\boldsymbol{\varphi}(t)$ from $\boldsymbol{\varphi}^*$ and of the output $\boldsymbol{y}(t)$ from $\boldsymbol{y}^*$, respectively; $\boldsymbol{L}_a = (l_{a_{ij}}) \in \mathbb{R}^{n\times n}$ is the Laplacian matrix such that

$$l_{a_{ij}} = \begin{cases} -l_{ij}\cos(\varphi_i^* - \varphi_j^*), & i \neq j,\\ \sum_{k\neq i} l_{ik}\cos(\varphi_i^* - \varphi_k^*), & i = j,\end{cases}$$

$\boldsymbol{B} = \mathrm{diag}(b_i) \in \mathbb{R}^{n\times n}$ is a diagonal matrix, $\boldsymbol{w} = \mathrm{col}(w_i) \in \mathbb{R}^n$ is Gaussian white noise, and $\boldsymbol{C} = (C_{ik}) \in \mathbb{R}^{n\times m}$ is the incidence matrix of the graph $\mathcal{G}$ such that

$$C_{ik} = \begin{cases} 1, & \text{node } i \text{ is the begin of edge } e_k,\\ -1, & \text{node } i \text{ is the end of edge } e_k,\\ 0, & \text{otherwise,}\end{cases} \tag{10}$$

where the direction of the edge e_k is specified as in the definition of y_k in (6). Because $\boldsymbol{L}_a$ is symmetric and non-negative definite, there exists an orthogonal matrix $\boldsymbol{U} \in \mathbb{R}^{n\times n}$ such that

$$\boldsymbol{U}^\top\boldsymbol{L}_a\boldsymbol{U} = \boldsymbol{\Lambda}, \tag{11}$$

where $\boldsymbol{\Lambda} = \mathrm{diag}(\lambda_i) \in \mathbb{R}^{n\times n}$ with $0 = \lambda_1 \le \lambda_2 \le \cdots \le \lambda_n$ being the eigenvalues of matrix $\boldsymbol{L}_a$. The orthogonal matrix $\boldsymbol{U}$ can be written as $\boldsymbol{U} = [\boldsymbol{u}_1, \boldsymbol{U}_2]$, where $\boldsymbol{u}_1 = \eta\boldsymbol{1}_n$, η is a constant, and $\boldsymbol{U}_2 = [\boldsymbol{u}_2, \ldots, \boldsymbol{u}_m] \in \mathbb{R}^{n\times(n-1)}$, with the ith column $\boldsymbol{u}_i$ of $\boldsymbol{U}$ being the eigenvector corresponding to the eigenvalue λ_i for $i = 2, \ldots, n$.

Due to the Gaussian distribution of $\boldsymbol{w}$, the state $\widehat{\boldsymbol{\varphi}}$ and the output $\widehat{\boldsymbol{y}}$ are also Gaussian, i.e.,

$$\widehat{\boldsymbol{\varphi}}(t) \in G\big(\boldsymbol{m}_{\widehat{\varphi}}(t), \boldsymbol{Q}_{\widehat{\varphi}}(t)\big),\ \widehat{\boldsymbol{y}}(t) \in G\big(\boldsymbol{m}_y(t), \boldsymbol{Q}_{\widehat{y}}(t)\big),$$

with $\boldsymbol{m}_{\widehat{\varphi}}(t) \in \mathbb{R}^n, \boldsymbol{Q}_{\widehat{\varphi}}(t) \in \mathbb{R}^{n\times n}$ and $\boldsymbol{m}_{\widehat{y}}(t) \in \mathbb{R}^m, \boldsymbol{Q}_{\widehat{y}}(t) \in \mathbb{R}^{m\times m}$. Because the system matrix in (9) is singular, the invariant probability distribution of $\widehat{\boldsymbol{\varphi}}(t)$ does not exist. See Appendix B for the invariant distribution of a linear stochastic system. In order to obtain the invariant probability of the output $\widehat{\boldsymbol{y}}(t)$, we make the following transformation. Let $\boldsymbol{x}(t) = \boldsymbol{U}^\top\widehat{\boldsymbol{\varphi}}(t)$. With spectral decomposition of $\boldsymbol{L}_a$ in (11), we obtain

$$\dot{\boldsymbol{x}}(t) = -\boldsymbol{\Lambda}\boldsymbol{x}(t) + \boldsymbol{U}^\top\boldsymbol{B}\boldsymbol{w}(t). \tag{12}$$

Decompose the state $\boldsymbol{x}(t)$ and the matrix $\boldsymbol{\Lambda}$ into block matrices,

$$\boldsymbol{x}(t) = \begin{bmatrix} x_1(t)\\ \boldsymbol{x}_2(t)\end{bmatrix},\ \boldsymbol{\Lambda} = \begin{bmatrix} 0 & \boldsymbol{0}\\ \boldsymbol{0} & \boldsymbol{\Lambda}_{n-1}\end{bmatrix} \in \mathbb{R}^{n\times n},$$

where $\boldsymbol{\Lambda}_{n-1} \in \mathbb{R}^{(n-1)\times(n-1)}$ is a diagonal matrix with all the diagonal elements being the nonzero eigenvalues of the matrix $\boldsymbol{L}_a$. With these block matrices, it yields from (12) that

$$\dot{\boldsymbol{x}}_2(t) = -\boldsymbol{\Lambda}_{n-1}\boldsymbol{x}_2(t) + \boldsymbol{U}_2^\top\boldsymbol{B}\boldsymbol{w}(t). \tag{13}$$

The output $\widehat{\boldsymbol{y}}(t)$ becomes

$$\widehat{\boldsymbol{y}}(t) = \boldsymbol{C}^\top\widehat{\boldsymbol{\varphi}} = \boldsymbol{C}^\top\boldsymbol{U}\boldsymbol{x}(t) = \big[\boldsymbol{C}^\top\boldsymbol{u}_1\boldsymbol{C}^\top\boldsymbol{U}_2\big]\boldsymbol{x}(t) = \boldsymbol{C}^\top\boldsymbol{U}_2\boldsymbol{x}_2(t),$$

where $\boldsymbol{C}^\top\boldsymbol{u}_1 = \eta\boldsymbol{C}^\top\boldsymbol{1} = \boldsymbol{0}$ is used. Hence, the output is independent of the component x_1. Because the system matrix, which equals to $-\boldsymbol{\Lambda}_{n-1}$, is Hurwitz, there exists an invariant probability distribution for the state $\boldsymbol{x}_2(t)$, with the expectation $\boldsymbol{m}_{x_2} = 0$ and the variance matrix $\boldsymbol{Q}_2 = (q_{2,ij}) \in \mathbb{R}^{(n-1)\times(n-1)}$ satisfying the Lyapunov equation,

$$\boldsymbol{0} = -\boldsymbol{\Lambda}_{n-1}\boldsymbol{Q}_2 - \boldsymbol{Q}_2\boldsymbol{\Lambda}_{n-1} + \boldsymbol{U}_2^\top\boldsymbol{B}\boldsymbol{B}^\top\boldsymbol{U}_2. \tag{14}$$

From the above equation, we further derive the analytic solution of $\boldsymbol{Q}_2$,

$$q_{2,ij} = (\lambda_{i+1} + \lambda_{j+1})^{-1}\boldsymbol{u}_{i+1}^\top\boldsymbol{B}\boldsymbol{B}^\top\boldsymbol{u}_{j+1}, i, j = 1, 2, \ldots, n-1. \tag{15}$$

Because of the dependence on the state $\boldsymbol{x}_2$, there also exists an invariant probability distribution for the output $\widehat{\boldsymbol{y}}(t)$ with the expectation $\boldsymbol{m}_{\widehat{y}} = \boldsymbol{0}$ and variance matrix

$$\boldsymbol{Q}_{\widehat{y}} = \boldsymbol{C}^\top\boldsymbol{U}_2\boldsymbol{Q}_2\boldsymbol{U}_2^\top\boldsymbol{C}. \tag{16}$$

Next, we consider the first hitting time of the state hitting the boundary of the secure domain in the system (5). Clearly, in a fixed interval of time, the higher the probability that the state stays in the secure domain (3), the larger the mean first hitting time is. Here, instead of the probability density function of the non-linear stochastic process (5), we focus on the invariant probability distribution of a linear stochastic process, which is defined as

$$\widetilde{\boldsymbol{y}} = \widehat{\boldsymbol{y}}(t) + \boldsymbol{y}^*, \tag{17}$$

where $\widehat{\boldsymbol{y}}$ is the output of the system (9). It is remarked that $\widetilde{\boldsymbol{y}}(t)$ approximates $\boldsymbol{y}(t)$ at the neighborhood of $\boldsymbol{y}^*$ due to the linearization of the system (5) at the synchronous state $\boldsymbol{\varphi}^*$ with $\boldsymbol{w}(t)$ dealt as an input to the system. Because $\boldsymbol{y}^*$ is a constant vector, the stochastic process $\widetilde{\boldsymbol{y}}$ is also Gaussian such that

$$\widetilde{\boldsymbol{y}}(t) \in G\big(\boldsymbol{m}_{\widetilde{y}}(t), \boldsymbol{Q}_{\widetilde{y}}(t)\big), \tag{18}$$

$$\boldsymbol{m}_{\widetilde{y}}(t) = \boldsymbol{m}_{\widehat{y}}(t) + \boldsymbol{y}^*,\ \boldsymbol{Q}_{\widetilde{y}}(t) = \boldsymbol{Q}_{\widehat{y}}(t). \tag{19}$$

Thus, there exists an invariant probability for the Gaussian process $\widetilde{\boldsymbol{y}}(t)$ in (18) with

$$\boldsymbol{m}_{\widetilde{y}}(t) = \boldsymbol{y}^*,\ \boldsymbol{Q}_{\widetilde{y}}(t) = \boldsymbol{Q}_{\widehat{y}}, \forall t \in \mathbb{T}.$$

If $\widetilde{\boldsymbol{y}}(0) \in G(\boldsymbol{y}^*, \boldsymbol{Q}_{\widehat{y}})$, the process of $\widetilde{\boldsymbol{y}}(t)$ is a stationary process, in which $\widetilde{\boldsymbol{y}}(t)$ fluctuates around its expectation $\boldsymbol{y}^*$ with variance matrix $\boldsymbol{Q}_{\widehat{y}}$. If $\widetilde{\boldsymbol{y}}(0) \notin G(\boldsymbol{y}^*, \boldsymbol{Q}_{\widehat{y}})$, the distribution of $\widetilde{\boldsymbol{y}}(t)$ will converge to the invariant distribution $G(\boldsymbol{y}^*, \boldsymbol{Q}_{\widehat{y}})$. Note that with sufficient small disturbances in a short time period, the process $\boldsymbol{y}(t)$ defined by (5) and (6) also fluctuates in the neighborhood of $\boldsymbol{y}^*$. Because $\widetilde{\boldsymbol{y}}(t)$ is an approximation of $\boldsymbol{y}(t)$, the variance matrix $\boldsymbol{Q}_{\widehat{y}}$ can be used to characterize the magnitude of the fluctuations of $\boldsymbol{y}(t)$.

As shown in (16), the variance matrix of the phase difference is determined by the network topology and the spectrum of the Laplacian matrix. Due to the dependence of the Laplacian matrix on the

natural frequency and the coupling strength, the variance matrix also depends on these parameters. In addition, in contrast to the expectation $\boldsymbol{y}^*$, the variance matrix $\boldsymbol{Q}_{\widetilde{y}}$ depends on the strength of the noise. Here, the trace of the matrix $\boldsymbol{Q}_{\widetilde{y}}$ is the $\mathscr{H}_2$ norm of the linear system (9) where $\boldsymbol{w}(t)$ is seen as an input to the system. This $\mathscr{H}_2$ norm is often used to analyze the fluctuations of the system subjected to disturbances.[13–15] See the Appendix B for details of the $\mathscr{H}_2$ norm.

Remark 4.1. *Instead of the system (9), the following linear system:*

$$\begin{aligned}\dot{\overline{\boldsymbol{\varphi}}}(t) &= \boldsymbol{\omega} - \boldsymbol{L}\overline{\boldsymbol{\varphi}}(t) + \boldsymbol{B}\boldsymbol{w}(t),\\ \overline{\boldsymbol{y}}(t) &= \boldsymbol{C}^\top\overline{\boldsymbol{\varphi}}(t),\end{aligned} \tag{20}$$

may be studied to improve synchronization stability of the system (4) by increasing the probability that the state remains in the secure domain according to the invariant probability distribution. Here, $\boldsymbol{\omega} = \mathrm{col}(\omega_i) \in \mathbb{R}^n$, $\boldsymbol{L} \in \mathbb{R}^{n\times n}$ *is the Laplacian matrix of the weighted graph with weight* l_{ij} *for the edge* $(i,j) \in \mathscr{E}$, *which is different from the matrix* $\boldsymbol{L}_a$ *defined in (9),* $\boldsymbol{B}$ *and* $\boldsymbol{C}$ *are the same as the ones defined in (9). This system is derived from (5) by replacing the term* $\sin(\varphi_i - \varphi_j)$ *by* $(\varphi_i - \varphi_j)$ *directly.*

In fact, the expectation of the phase difference satisfies

$$\overline{\boldsymbol{y}}^* = \boldsymbol{C}^\top\boldsymbol{L}^\dagger\boldsymbol{\omega}, \tag{21}$$

where $\boldsymbol{L}^\dagger$ *is the Moore–Penrose inverse of* $\boldsymbol{L}$. *The matrix* $\boldsymbol{L}$ *has the following spectral decomposition:*

$$\boldsymbol{V}^\top\boldsymbol{L}\boldsymbol{V} = \boldsymbol{\Gamma},$$

where $\boldsymbol{\Gamma} = \mathrm{diag}(\gamma_i) \in \mathbb{R}^{n\times n}$ *with* γ_i *being the eigenvalue of the matrix* $\boldsymbol{L}$ *and the column vector* $\boldsymbol{v}_i$ *of* $\boldsymbol{V}$ *being the eigenvector of* $\boldsymbol{L}$ *corresponding to the eigenvalue* σ_i. *Since* $\boldsymbol{L}\boldsymbol{1} = \boldsymbol{0}$, $\gamma_1 = 0$ *is an eigenvalue with eigenvector* $\boldsymbol{v}_1 = \tau\boldsymbol{1}$. *Similar to the matrix* $\boldsymbol{U}$ *in (11),* $\boldsymbol{V}$ *is rewritten as* $\boldsymbol{V} = [\boldsymbol{v}_1, \boldsymbol{V}_2]$ *with* $v_1 = \tau\boldsymbol{1} \in \mathbb{R}^n$ *and* $\boldsymbol{V}_2 = [\boldsymbol{v}_2, \ldots, \boldsymbol{v}_n] \in \mathbb{R}^{n\times(n-1)}$. *The variance matrix of the output satisfies*

$$\overline{\boldsymbol{Q}}_y = \boldsymbol{C}^\top\boldsymbol{V}_2\overline{\boldsymbol{Q}}_2\boldsymbol{V}_2^\top\boldsymbol{C}, \tag{22}$$

where $\overline{\boldsymbol{Q}}_2 = (\overline{q}_{2,ij}) \in \mathbb{R}^{(n-1)\times(n-1)}$ *such that*

$$\overline{q}_{2,ij} = (\gamma_{i+1} + \gamma_{j+1})^{-1}\boldsymbol{v}_{i+1}^\top\boldsymbol{B}\boldsymbol{B}^\top\boldsymbol{v}_{j+1}, i,j = 1,\ldots,n-1. \tag{23}$$

The invariant probability distribution can also be obtained with the expectation in (21) and the variance in (22).

However, in the invariant distribution, $\overline{\boldsymbol{y}}(t)$ *fluctuates around* $\overline{\boldsymbol{y}}^*$ *calculated from (21), which is obviously different from* $\boldsymbol{y}^*$ *at the synchronous state (2) and this difference increases as the synchronous state of the system (4) moves to the boundary of the secure domain. In addition, because of the independence of* $\boldsymbol{V}$ *and* $\boldsymbol{\Gamma}$ *on the synchronous state, the variance matrix* $\overline{\boldsymbol{Q}}_y$ *in (22) is independent of the synchronous state. This is different from the variance matrix* $\boldsymbol{Q}_{\widetilde{y}}$ *in (16), which depends the eigenvalues of the matrix* $\boldsymbol{L}_a$ *that yields from linearization at the synchronous state. Due to this independence, the nonlinearity of the system (4) cannot be reflected by the probability of the state being absent from the secure domain at the invariant probability distribution of the process (20).*

V. THE OPTIMIZATION FRAMEWORK

To increase the mean first time of the state hitting the boundary of the secure domain, a way is to increase the probability of the state staying in the domain. Since $\widetilde{\boldsymbol{y}}$ is an approximation of $\boldsymbol{y}(t)$ at the neighborhood of $\boldsymbol{y}^*$ and the distribution of $\widetilde{\boldsymbol{y}}(t)$ will converge to its invariant distribution, we focus on the probability of the process $\widetilde{\boldsymbol{y}}(t)$ staying in the secure domain in the invariant distribution. However, this probability can hardly be computed in practice due to an integral over a supercube of dimension m, which involves immense computational complexity. Thus, we focus on the components of $\widetilde{\boldsymbol{y}}(t)$, which are the stochastic process of phase differences in the edges. In the invariant probability distribution, for edge e_k, the expectation and the variance of the phase difference are denoted by μ_k and σ_k^2, respectively, which are computed as

$$\mu_k = y_k^*,\ \sigma_k^2 = q_{kk},\ \text{for } k = 1,\ldots,m, \tag{24}$$

where y_k^* is the phase difference at the synchronous state that can be calculated from (7), q_{kk} is the kth diagonal element of the matrix $\boldsymbol{Q}_{\widetilde{y}}$ which is solved from (16). The probability that the phase difference $\widetilde{y}_k(t)$ in edge e_k belongs to the secure domain according to the invariant probability distribution is

$$s_k(\mu_k,\sigma_k) = \int_{-\frac{\pi}{2}}^{\frac{\pi}{2}} \frac{1}{\sigma_k\sqrt{2\pi}} e^{\frac{-(x-\mu_k)^2}{2\sigma_k^2}}\,\mathrm{d}x. \tag{25}$$

Hence, the probability according to invariant probability distribution that the phase difference of the process $\widetilde{y}_k(t)$ is outside the secure domain is equal to

$$p_k(\mu_k,\sigma_k) = 1 - s_k(\mu_k,\sigma_k), \tag{26}$$

for edge e_k for $k = 1,\ldots,m$. Due to the approximation of the process (17) to the output process of system (5), this value measures the risk of the phase difference in edge e_k of the system (5) exceeding $\pi/2$. Thus, by this value, the vulnerable edges at which the system loses synchronization can be identified. Based on this value, we use the $\mathscr{L}_\infty$ norm of the vector $\boldsymbol{P}(\boldsymbol{\mu},\boldsymbol{\sigma})$ to measure the risk of the state hitting the boundary of the secure domain, i.e.,

$$\boldsymbol{P}(\boldsymbol{\mu},\boldsymbol{\sigma}) = \mathrm{col}\big(p_k(\mu_k,\sigma_k)\big) \in \mathbb{R}^m, \tag{27a}$$

$$||\boldsymbol{P}(\boldsymbol{\mu},\boldsymbol{\sigma})||_\infty = \max_{k=1,\ldots,m}\{p_k(\mu_k,\sigma_k)\}, \tag{27b}$$

where $\boldsymbol{\mu} = \mathrm{col}(\mu_k) \in \mathbb{R}^m$ and $\boldsymbol{\sigma} = \mathrm{col}(\sigma_k) \in \mathbb{R}^m$. Clearly, the risk of losing synchronization increases as the probability of the phase difference presenting outside of the secure domain. Thus, this norm also measures the risk of the system losing synchronization.

The following proposition describes the ranges of this norm and its relationship with the second smallest eigenvalue of the matrix $\boldsymbol{L}_a$, which is often used to study the linear stability of the complex system (1).[7,10]

Proposition 5.1. *Consider the invariant probability distribution of the processes* $\widetilde{\boldsymbol{y}}(t)$ *of the phase differences in the edges defined in (17). It holds that*

(1) *the norm* $||\boldsymbol{P}(\boldsymbol{\mu},\boldsymbol{\sigma})||_\infty$ *ranges over the interval* $[0,1]$,
(2) *if the second smallest eigenvalue of the matrix* $\boldsymbol{L}_a$ *decreases to zero, then the norm* $||\boldsymbol{P}(\boldsymbol{\mu},\boldsymbol{\sigma})||_\infty$ *defined in (27) increases to the value 1.*

Proof.

(1) At a synchronous state, when the strength of the disturbances vary from zero to infinity, for $k = 1, \ldots, m$, the variance σ_k for edge e_k varies from zero to infinity. Following from (25) and (26), the range of $p_k(\mu_k, \sigma_k)$ is $[0, 1]$; thus, this norm also lies in $[0, 1]$.

(2) For $\boldsymbol{A}, \boldsymbol{B} \in \mathbb{R}^{n\times n}$, we say that $\boldsymbol{A} \preceq \boldsymbol{B}$ if the matrix $\boldsymbol{A} - \boldsymbol{B}$ is semi-negative definite. Define $\underline{b} = \min\{b_i, i = 1, \ldots, n\}$. Then,

$$\boldsymbol{B}\boldsymbol{B}^\top \succeq \underline{b}^2 \boldsymbol{I}_n,$$

where $\boldsymbol{I}_n \in \mathbb{R}^{n\times n}$ is an identity matrix. From (14) and (16), we derive

$$\boldsymbol{Q}_2 \succeq \frac{1}{2}\underline{b}^2 \boldsymbol{\Lambda}_{n-1}^{-1}, \ \boldsymbol{Q}_{\tilde{y}} \succeq \frac{1}{2}\underline{b}^2 \boldsymbol{C}^\top \boldsymbol{U}_2 \boldsymbol{\Lambda}_{n-1}^{-1} \boldsymbol{U}_2^\top \boldsymbol{C}.$$

To prove this proposition, we only need to prove that as the second smallest eigenvalue decreases to zero, there is at least one diagonal element of the matrix $\boldsymbol{S} = \boldsymbol{C}^\top \boldsymbol{U}_2 \boldsymbol{\Lambda}_{n-1}^{-1} \boldsymbol{U}_2^\top \boldsymbol{C}$ that increases to infinity. The incidence matrix of the graph is written into $\boldsymbol{C} = [\boldsymbol{c}_1 \boldsymbol{c}_2 \cdots \boldsymbol{c}_m]$, where the vector $\boldsymbol{c}_k$ describes the indices of the two nodes that are connected by edge e_k. Without losing generality, assume the direction of edge e_k is from node i to j. Then, ith and jth elements of the vector $\boldsymbol{C}_k$, $c_{ik} = 1$ and $c_{jk} = -1$, respectively and the other elements all equal to zero. From the definition of the matrix $\boldsymbol{S}$, we obtain the diagonal element of $\boldsymbol{S}$,

$$s_{kk} = \sum_{q=1}^{m-1} \lambda_{q+1}^{-1} (u_{i,q+1} - u_{j,q+1})^2, \ k = 1, 2 \cdots m,$$

where $u_{i,q+1}$ and $u_{j,q+1}$ are ith and jth elements of the vector $\boldsymbol{u}_{q+1}$ and $\boldsymbol{u}_{q+1}$ is the $(q+1)$th column of the matrix $\boldsymbol{U}$ defined in (11). Because $\boldsymbol{u}_2$ is the second column of the orthogonal matrix $\boldsymbol{U}$, which is the eigenvector of $\boldsymbol{L}_a$ corresponding to the second smallest eigenvalue λ_2, there exist i, j with $i \neq j$ such that $u_{i,2} \neq u_{j,2}$; thus, s_{kk} increases to infinity as the second smallest eigenvalue λ_2 decreases to zero.

□

As natural frequencies increase or the coupling strength of the edges decrease, the synchronous state will move toward the boundary of the secure domain. In this case, the basin of attraction of the synchronous state gradually disappears and the second smallest eigenvalue of $\boldsymbol{L}_a$ decreases to zero. Because the norm $||\boldsymbol{P}(\boldsymbol{\mu}, \boldsymbol{\sigma})||_\infty$ increases to its upper bound as the second smallest eigenvalue of $\boldsymbol{L}_a$ decreases to zero when the synchronous state disappears, it fully indicates the response of linear stability and nonlinear stability to these system parameters. Besides this property, the value $\boldsymbol{P}(\boldsymbol{\mu}, \boldsymbol{\sigma})$ also depends on the strength of the noise due to the dependence of $\boldsymbol{\sigma}$ on the strength of the noise. This is different from the spectrum of the system matrix and the size of the basin of attraction, which are independent of the strength of the noise. In addition, with the elements in the vector $\boldsymbol{P}(\boldsymbol{\mu}, \boldsymbol{\sigma})$, the response of the vulnerability of each edge to the changes of the system parameters can be captured. Thus, this metric is more practical and comprehensive for the analysis of synchronization stability.

With the metric $||\boldsymbol{P}(\boldsymbol{\mu}, \boldsymbol{\sigma})||_\infty$, we propose an optimization framework to increase the mean first hitting time and, thus, enhance synchronization stability. In this optimization framework, the objective is minimizing the risk of the state hitting the boundary of the secure domain and the decision variables include the coupling strength and the natural frequency.

We first study the effects of the coupling strength given the natural frequency and the network topology. It is well known that synchronization stability increases as the coupling strength of the edges increase. Thus, we consider the networks with a constant total amount of coupling strengths. Consider the system (5), the optimization problem for the assignment of the coupling strength is

$$\min_{l_{ij}\in\mathbb{R},(i,j)\in\mathcal{E}} ||\boldsymbol{P}(\boldsymbol{\mu}, \boldsymbol{\sigma})||_\infty,$$

$$\text{s.t. } (2), (7), (11), (15), (16), (24), \tag{28a}$$

$$0 = \sum_{(i,j)\in\mathcal{E}} l_{ij} - W, \tag{28b}$$

$$\underline{l}_{ij} < l_{ij} < \bar{l}_{ij} \text{ for } (i,j) \in \mathcal{E}, \tag{28c}$$

where $W \in \mathbb{R}$ is the total amount of the coupling strength, and $\underline{l}_{ij} > 0$ and $\bar{l}_{ij} > 0$ are, respectively, the lower and upper bounds of the coupling strength of the edge. In this optimization problem, the coupling strength does not only impact the synchronous state but also the variance of phase differences, thus affecting synchronization stability in a non-linear way.

We next consider the assignment of the natural frequency given the coupling strength and network topology. Consider the system (5), the optimization problem for the design of the natural frequency is

$$\min_{\omega_i\in\mathbb{R},i\in\mathcal{V}} ||\boldsymbol{P}(\boldsymbol{\mu}, \boldsymbol{\sigma})||_\infty, \tag{29a}$$

$$\text{s.t. } (2), (7), (11), (15), (16), (24) \tag{29b}$$

$$0 = \sum_{i=1}^{n} \omega_i, \tag{29c}$$

$$\underline{\omega}_i < \omega_i < \overline{\omega}_i, i = 1, \ldots, n, \tag{29d}$$

where $\underline{\omega}_i$ and $\overline{\omega}_i$ are lower and upper bounds of ω_i, respectively.

In order to use the proposed metric $\boldsymbol{P}(\boldsymbol{\mu}, \boldsymbol{\sigma})$ to analyze synchronization stability of complex systems in practice, one has to solve the nonlinear equation (2) for the expectation $\boldsymbol{\mu}$ and perform the matrix spectral decomposition (11) for the variance matrix $\boldsymbol{Q}_{\tilde{y}}$, for which the Newton iterative method and the QR method can be used, respectively. In particular, if the QR method is used for matrix decomposition, the estimated computing complexity is $O(n^3)$. To solve corresponding optimization problems, iterative methods can be used, where the solution to (2) and the matrix spectral decomposition (11) are needed in each iteration. Thus, besides efficient algorithms for solving the non-linear equation (2) and for matrix spectral decomposition (11), an iterative method for optimization problems with a fast convergence rate is important for increasing synchronization stability of large-scale systems using the proposed optimization framework.

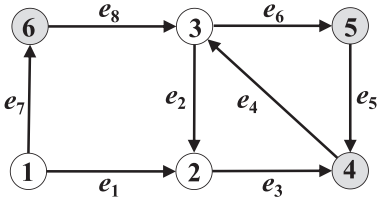

FIG. 1. A network with six nodes and eight edges.

VI. CASE STUDY

We evaluate the performance of the optimization framework for increasing synchronization stability. Monte-Carlo method-based numerical simulations are carried out to compute the mean first hitting time of the nonlinear stochastic system (5) and to identify the vulnerable edges in the network. By these simulations, we verify the effectiveness of the metric p_k in (26) on finding the vulnerable edges and of the optimization framework on increasing the first mean hitting time.

In simulations, we use the Euler–Maruyama method to discretize the system (5) with the simulation time T, the time step size dt, and the initial condition $\boldsymbol{\varphi}(0) = \boldsymbol{\varphi}^*$. If there is an edge in which the absolute value of the phase difference exceeds $\pi/2$, simulation is stopped. Then, the stopping time and the index of this edge are recorded. The mean first hitting time $\bar{t}_e$ is obtained as the mean of the stopping time in these simulations. In these simulations, only those simulations are counted that lead to a stopped process within the simulation horizon T. The total number of counted simulations is N which almost equals to the total number of simulations. In addition, the number g_k that the absolute value of the phase difference exceeding $\pi/2$ among simulations is counted for the edge e_k. For each line, we calculate the following ratio:

$$r_k = g_k/N, \tag{30}$$

which satisfies $\sum_{k=1}^{m} r_k = 1$. This ratio approximates the probability that the absolute value of the phase difference exceeds $\pi/2$ at line e_k conditioned on that the state exits the secure domain. Clearly, the larger the ratio for an edge, the easier the boundary of the secure domain is hit by the phase difference at this edge. The risk of the phase difference exceeding $\pi/2$ at each edge is calculated from (26). To compare with the ratio r_k, we calculate the value

$$\widetilde{p}_k = \frac{p_k}{\sum_j^m p_j}, \text{ for } k = 1, \ldots, m, \tag{31}$$

which is the probability of the absolute value of the phase difference exceeding $\pi/2$ in edge e_k conditioned on the state being absent from the secure domain in the invariant probability distribution of the linear stochastic process (17).

Regarding the effectiveness of the optimization framework in the enhancement of the synchronization stability, we compare the solutions of the following five optimization frameworks,

(1) Maximizing the order parameter r at the synchronous state of the system (1),[9] see the optimization problems (A1) and (A2) in Appendix A;
(2) Minimizing the $\mathscr{L}_\infty$ norm of phase differences at the synchronous state, which aims to increase the phase cohesiveness of the system (1),[8] see the optimization problems (A3) and (A4) in Appendix A;
(3) Minimizing the $\mathscr{L}_\infty$ norm of the variance of the phase differences in the invariant probability distribution of the process (17), which aims to decrease the fluctuations in the phase differences of the system (1) with disturbances. The corresponding optimization problems can be obtained by replacing the objective functions in (28) and (29) by $||\boldsymbol{\sigma}||_\infty$;
(4) Minimizing the $\mathscr{H}_2$ norm of the system (9), which aims to decrease the fluctuations in the phase differences of the system (1) with disturbances, see the optimization problems (A5) and (A6) in Appendix A; and
(5) Minimizing the risk of the state hitting the boundary of the secure domain measured by $||\boldsymbol{P}||_\infty$, see the optimization problems (28) and (29).

In the first two optimization frameworks, the focuses of the objectives are on the synchronous state of the deterministic system (1) where the impacts of disturbances are not considered. However, in the latter three optimization frameworks, the disturbances are involved in while the synchronous state is not fully considered. Note that by the metric of the phase cohesiveness, the vulnerable edges may be identified as the ones in which the phase differences are large, while by the metric of the variance of the phase difference, the vulnerable edges may also be identified as the ones in which the variances are large.[16] The optimization problems are solved by Matlab.

We evaluate the performance of the proposed optimization framework for increasing the synchronization stability in the two networks shown in Figs. 1 and 5 respectively. By the network in Fig. 1, we show the relationship between the metric $\|P\|_\infty$ and the mean first hitting time $\bar{t}_e$ and the performance of the vector $\boldsymbol{P}(\boldsymbol{\mu}, \boldsymbol{\sigma})$ on identifying the vulnerable lines. In addition, by presenting the solutions of the corresponding optimization problems for the design of the coupling strength and the natural frequency, we show the performance of the proposed optimization framework on increasing the mean first hitting time. By the network in Fig. 5, we confirm the performance of the proposed optimization framework for relatively large-scale systems.

Example 6.1. *Consider the network in Fig. 1 with six nodes and eight edges. The natural frequencies at gray nodes are negative while those at other nodes are positive. The directions of the edges are specified arbitrary, which do not affect the analysis. We set* $T = 10^5$, $\mathrm{dt} = 10^{-3}$, $N = 10^5$, $b_i = 1.05$ *for all the nodes. We formulate an Initial Model, in which we set* $\omega_i = 5$ *for* $i = 1, 2, 3$ *and* $\omega_i = -5$ *for* $i = 4, 5, 6$ *and* $l_{ij} = 8$ *for all the edges. In the optimization problems for the design of the coupling strength, we set* $\omega_i = 5$ *for* $i = 1, 2, 3$, *and* $\omega_i = -5$ *for* $i = 4, 5, 6$, *the total coupling strength* $W = 64$ *and* $\underline{l}_{ij} = 1$, $\bar{l}_{ij} = 12$ *for all the edges. In the optimization problems for the design of the natural frequency, we set* $\underline{\omega}_i = -5$ *and* $\bar{\omega}_i = -5$ *for nodes* 4, 5, 6 *and* $\underline{\omega}_i = 0$ *and* $\bar{\omega}_i = 15$ *for nodes* 1, 2, 3, *and* $l_{ij} = 8$ *for all the edges.*

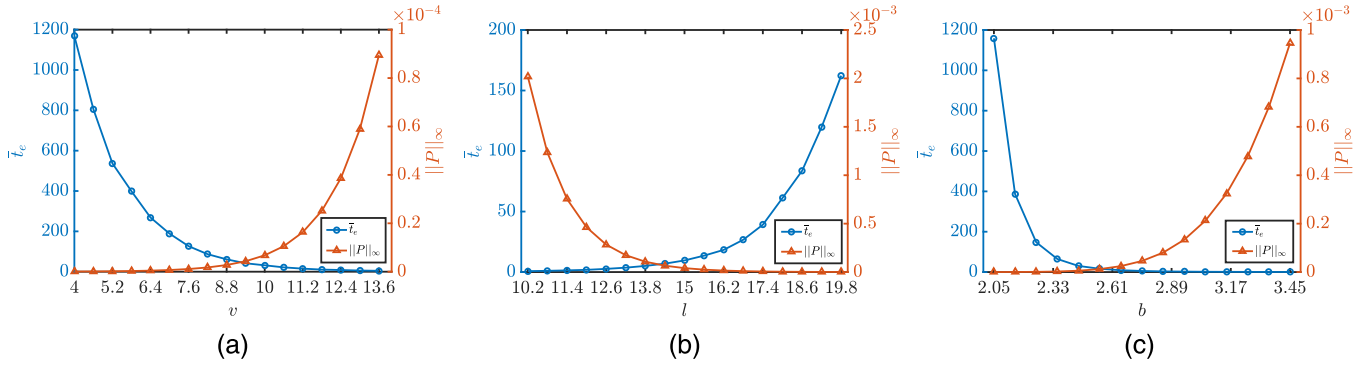

FIG. 2. The dependence of the mean first time $\bar{t}_e$ and the defined metric $\|P\|_\infty$ on the system parameters. (a) $\omega_i = v$ for $i = 1, 2, 3$ and $\omega_i = -v$ for $i = 4, 5, 6$ where v is a positive constant, $l_{ij} = 22$ for all the edges, and $b_i = 2.1$ for all the nodes. (b) $\omega = 5$ for $i = 1, 2, 3$ and $\omega = -5$ for $i = 4, 5, 6$ and $l_{ij} = l$ for all the edges where l is a positive constant, $b_i = 2.1$ for all the nodes. (c) $\omega = 5$ for $i = 1, 2, 3$ and $\omega = -5$ for $i = 4, 5, 6$ and $l_{ij} = 22$ for all the edges where b is a positive constant and $b_i = b$ for all the nodes.

We first focus on the relationship between the mean first hitting time and the risk of the state hitting the boundary of the secure domain measured by $||\boldsymbol{P}||_\infty$. Shown in Fig. 2 are the dependence of the mean first hitting time and $||\boldsymbol{P}||_\infty$ on the natural frequency, the coupling strength and the disturbances. The configuration of the parameters are described in the caption of Fig. 2. It is demonstrated that as the risk of the state hitting the boundary of the secure domain increases, the mean first hitting time decreases. This indicates that synchronization stability decreases. It can be imagined that as the risk of the state hitting the boundary of the secure domain increases to one, the mean first hitting time will decrease to zero.

Next, we consider the identification of the vulnerable edges in the system (5) by the metric defined in (26) in the network. The values r_k and $\widetilde{p}_k$ for each edge are shown in Fig. 3. It is demonstrated that $\widetilde{p}_k$ estimates r_k well for all the edges and e_7 is the most vulnerable edge. Thus, the vulnerability of the edge can be measured by the metric p_k.

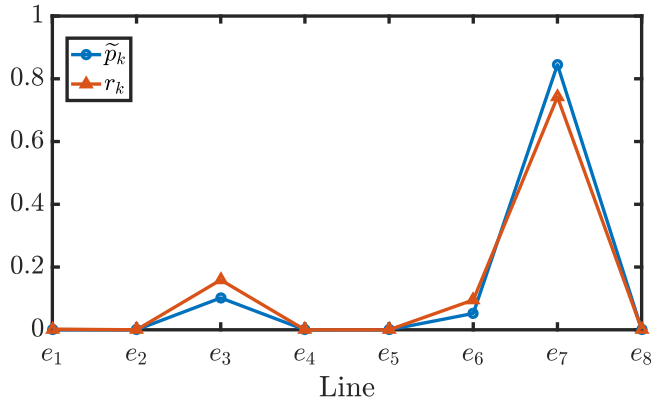

FIG. 3. The value $\widetilde{p}_k$ and the ratio r_k at the edges. We set $\omega_i = 5$ for $i = 1, 2, 3$, $\omega_i = -5$ for $i = 4, 5, 6$, $l_{ij} = 20$ for all the edges, and $b_i = 2.1$ for all the nodes.

Let us investigate the optimal distribution of the coupling strength. Table I shows the optimal solution for the design of coupling strength by optimization problems with the five objectives. It can be seen that the mean first hitting time increases from 118.46 to 363.396, 773.220, and 3951.733 s by minimizing the largest variance of phase differences measured by $||\boldsymbol{\sigma}||_\infty$, the $\mathscr{H}_2$ norm, and the risk of the state hitting the secure domain measured by $||\boldsymbol{P}||_\infty$, respectively. It demonstrates that by suppressing the variance of phase differences, i.e., minimizing the $\mathscr{H}_2$ norm or $||\boldsymbol{\sigma}||_\infty$, the mean first hitting time can be effectively increased. However, this is insufficient when compared with the one minimizing $||\boldsymbol{P}||_\infty$, which as shown is the most effective way to increase the mean first hitting time. This is because both the synchronous state determined in the deterministic system and the variance of phase differences determined in a stochastic system are considered in the objective of $||\boldsymbol{P}||_\infty$. In addition, it is found that the mean first hitting time decreases to 39 and 57.631 s in the solution to the first two optimization problems, respectively. In other words, maximizing the order parameter or the phase cohesiveness may decrease synchronization stability. Hence, *a larger order parameter or a higher level phase cohesiveness does not mean that the system is more robust against disturbances and it may not be wise to design the coupling strength of the network with disturbances so as to maximize these objectives.*

It is seen in Table II for the solution to the five optimization problems that the most vulnerable edges that have the largest value of r_k are e_8, e_1, e_3, e_7, and e_8, respectively. Clearly, these edges have been identified by the defined value $\widetilde{p}_k$. Figure 4 shows the fluctuations of the phase differences around the values at the synchronous state at time 10–15s in the initial model and the five most vulnerable edges after designing the coupling strength with five different objectives, respectively. It is shown in Figs. 4(a)–4(c) that the phase differences at the synchronous state, which are denoted by dashed red lines, are effectively decreased by either maximizing the order parameter or the phase cohesiveness. However, the variance of the phase difference is unexpectedly increased which leads to a high risk of the state hitting the boundary of the secure domain and a smaller mean first hitting time. This is also demonstrated by the data in

TABLE I. The coupling strength l_{ij}, the expectations μ_k, and the variances σ_k^2 of the phase differences, the value $\widetilde{p}_k$ defined in (31), the value r_k defined in (30), the mean first hitting time $\bar{t}_e$, and the values of objective functions in the initial model and in the solutions of five optimization problems with respect to the design of the coupling strength of the network in Fig. 1.

		e_1	e_2	e_3	e_4	e_5	e_6	e_7	e_8	r	$\|\|\boldsymbol{\mu}\|\|_\infty$	$\|\|\boldsymbol{\sigma}\|\|_\infty$	$\mathscr{H}_2$	$\|\|\boldsymbol{P}\|\|_\infty$	$\bar{t}_e$
Init. model	l_{ij}	8.000	8.000	8.000	8.000	8.000	8.000	8.000	8.000	0.9576	0.539	0.055	0.367	3.601e-6	118.460s
	μ_k	0.133	−0.248	0.539	−0.291	−0.176	0.467	0.514	−0.133						
	σ_k^2	0.051	0.038	0.045	0.036	0.045	0.046	0.055	0.051						
	$\widetilde{p}_k$	2.473×10^{-5}	1.192×10^{-6}	0.129	1.284×10^{-6}	4.909×10^{-6}	0.035	0.836	2.473×10^{-5}						
	r_k	0	0	0.179	0	0	0.070	0.751	0						
Max. r	l_{ij}	4.882	10.673	11.990	6.417	5.037	11.999	11.998	1.005	0.9805	0.407	0.147	0.481	2.806×10^{-4}	39.000s
	μ_k	0.051	−0.107	0.350	−0.242	−0.129	0.371	0.407	−0.249						
	σ_k^2	0.096	0.033	0.033	0.036	0.051	0.038	0.047	0.147						
	$\widetilde{p}_k$	0.002	1.974×10^{-12}	4.253×10^{-8}	4.321×10^{-9}	3.363×10^{-7}	1.042×10^{-6}	1.319×10^{-4}	0.998						
	r_k	0.017	0	0	0	0	0	0.013	0.970						
Min. $\|\|\boldsymbol{\mu}\|\|_\infty$	l_{ij}	1.807	10.146	11.023	5.086	8.604	11.855	11.888	3.592	0.9740	0.402	0.136	0.474	9.637×10^{-5}	57.631s
	μ_k	0.196	−0.108	0.397	−0.289	−0.082	0.371	0.402	−0.098						
	σ_k^2	0.136	0.034	0.036	0.037	0.040	0.035	0.046	0.111						
	$\widetilde{p}_k$	0.948	1.310×10^{-11}	2.822×10^{-6}	1.071×10^{-7}	3.953×10^{-10}	7.339×10^{-7}	2.298×10^{-4}	0.052						
	r_k	0.870	0	0.001	0	0	0	0.011	0.118						
Min. $\|\|\boldsymbol{\sigma}\|\|_\infty$	l_{ij}	8.979	5.538	9.332	4.711	8.218	8.804	9.429	8.990	0.9625	0.533	0.048	0.364	4.955×10^{-7}	363.396s
	μ_k	0.108	−0.225	0.533	−0.308	−0.142	0.450	0.441	−0.108						
	σ_k^2	0.046	0.044	0.045	0.044	0.045	0.046	0.048	0.046						
	$\widetilde{p}_k$	7.622×10^{-6}	1.124×10^{-4}	0.720	0.001	1.196×10^{-5}	0.111	0.167	7.444×10^{-6}						
	r_k	0	0	0.661	0.003	0	0.129	0.207	0						
Min. $\mathscr{H}_2$	l_{ij}	8.112	6.111	9.660	5.739	7.600	9.080	9.586	8.112	0.9652	0.496	0.050	0.362	1.124×10^{-7}	773.220s
	μ_k	0.112	−0.217	0.496	−0.279	−0.155	0.435	0.441	−0.112						
	σ_k^2	0.050	0.042	0.042	0.040	0.046	0.044	0.048	0.050						
	$\widetilde{p}_k$	1.438×10^{-4}	7.541×10^{-5}	0.374	2.422×10^{-4}	8.899×10^{-5}	0.138	0.487	1.438×10^{-4}						
	r_k	0	0	0.383	0	0.001	0.158	0.458	0						
Min. $\|\|\boldsymbol{P}\|\|_\infty$	l_{ij}	7.489	4.881	11.713	3.972	7.489	11.035	11.719	5.701	0.9749	0.429	0.064	0.373	4.302×10^{-9}	3951.733s
	μ_k	0.091	−0.167	0.429	−0.261	−0.120	0.381	0.378	−0.120						
	σ_k^2	0.054	0.046	0.038	0.044	0.046	0.039	0.041	0.064						
	$\widetilde{p}_k$	0.011	0.003	0.229	0.023	6.564×10^{-4}	0.083	0.228	0.422						
	r_k	0.009	0.003	0.282	0.030	0.001	0.090	0.240	0.310						

TABLE II. The most vulnerable edges identified by four metrics in the initial model and in the solution of five optimization problems with respect to the design of the coupling strength for the network in Fig. 1.

	by μ_k	by σ_k	by p_k	by r_k
Init. model	e_3	e_7	e_7	e_7
Max. r	e_7	e_8	e_8	e_8
Min. $\|\|\boldsymbol{\mu}\|\|_\infty$	e_7	e_1	e_1	e_1
Min. $\|\|\boldsymbol{\sigma}\|\|_\infty$	e_3	e_7	e_3	e_3
Min. $\mathscr{H}_2$	e_3	e_1	e_7	e_7
Min. $\|\|\boldsymbol{P}\|\|_\infty$	e_3	e_8	e_8	e_8

TABLE III. The natural frequencies at node $i = 1, \ldots, 3$ in the initial model and in the solutions of five optimization problems with respect to the design of the natural frequency for the network in Fig. 1.

	ω_1	ω_2	ω_3
Init. model	5.000	5.000	5.000
Max. r	1.128	0.487	13.385
Min. $\|\|\boldsymbol{\mu}\|\|_\infty$	5.034	3.691	6.275
Min. $\|\|\boldsymbol{\sigma}\|\|_\infty$	2.621	2.720	9.660
Min. $\mathscr{H}_2$	2.503	2.977	9.520
Min. $\|\|\boldsymbol{P}\|\|_\infty$	1.765	6.395	6.840

Table I. In contrast, by comparing the plots in Figs. 4(d) and 4(e) with the one in Fig. 4(a), it is found that the variance in the phase difference is greatly decreased by minimizing the $\mathscr{H}_2$ norm and $||\boldsymbol{\sigma}||_\infty$, which, however, does not effectively decrease the absolute value of the phase differences at the synchronous state. This further leads to a smaller mean first hitting time compared with the solution of the proposed optimization method as shown in Table I. In particular, it is found that the fluctuations of the dynamics in Figs. 4(d) and 4(e) are much smaller than in Fig. 4(f), while the latter one have a longer mean first hitting time. *This indicates that smaller fluctuations in the phase difference do not mean stronger synchronization stability, where the expectation of the phase difference has to be considered.*

Let us consider the design of the natural frequency by five optimization frameworks. Table III shows the natural frequencies at nodes 1, 2, and 3 after solving five optimization problems. Table IV shows the values of the objectives, the mean first hitting time, and the values of $\mu_k, \sigma_k^2, \tilde{p}_k$, and r_k in the edge e_k for $k = 1, \ldots, m$. It is observed that minimizing the risk of the state hitting the boundary of the secure domain measured by $||\boldsymbol{P}||_\infty$ can effectively increase the mean first hitting time. When observing the order parameter r and $||\boldsymbol{\mu}||_\infty$, it is found again that *a larger order parameter or a smaller* $||\boldsymbol{\mu}||_\infty$ *does not mean stronger synchronization stability*. Hence, it is demonstrated again that considering the variance in phase differences only is insufficient for increasing synchronization stability.

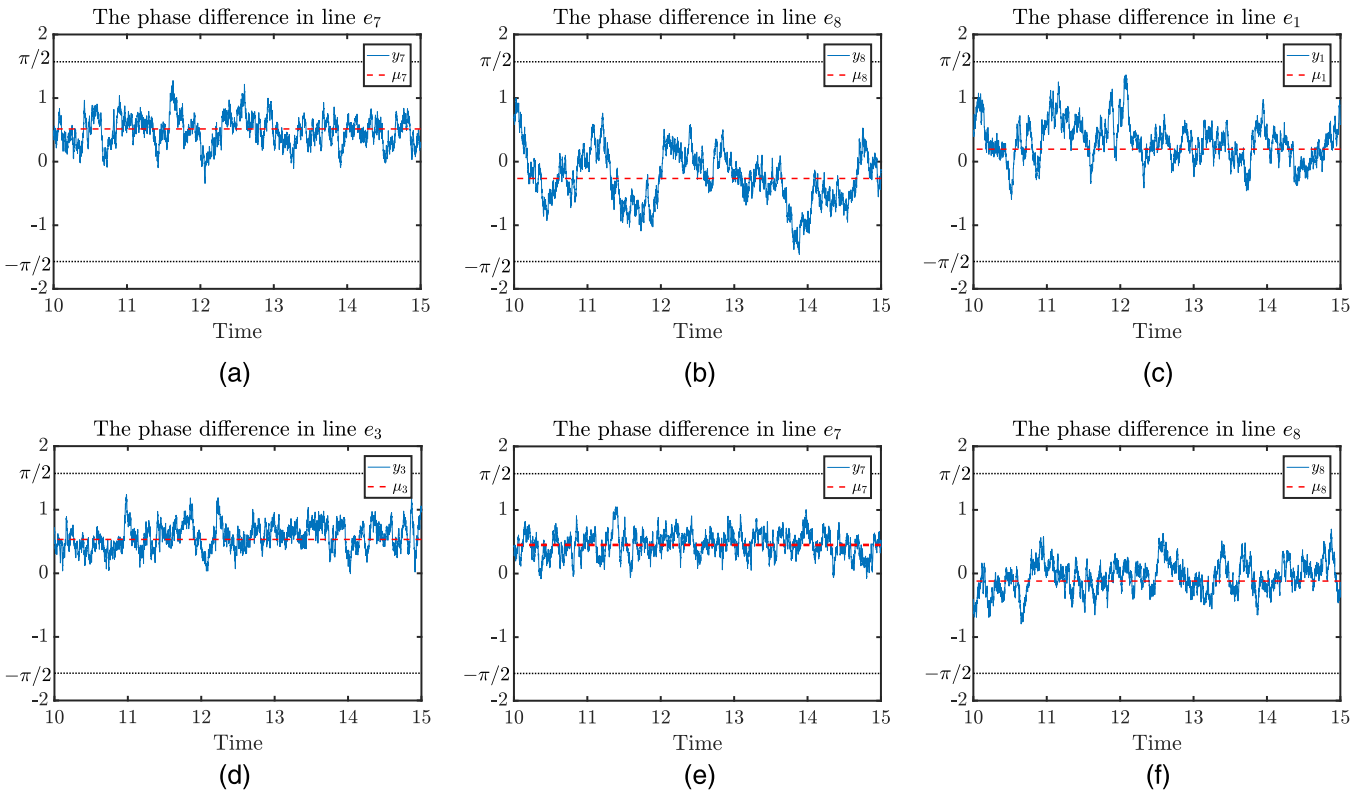

FIG. 4. The phase differences in the most vulnerable edges after designing the coupling strength with the five different objectives the network in Fig. 1. (a) Initial model. (b) Max. γ. (c) Min. $||\mu||_\infty$. (d) Min. $||\sigma||_\infty$. (e) Min. $\mathscr{H}_2$. (f) Min. $||\boldsymbol{P}||_\infty$.

TABLE IV. The expectations μ_k and the variances σ_k^2 of phase differences, the value $\widetilde{p}_k$ defined in (31), the value r_k defined in (30), the mean first hitting time $\bar{t}_e$, and the values of the objective functions in the initial model and in the solutions to five optimization problems with respect to the design of the natural frequency for the network in Fig. 1.

		e_1	e_2	e_3	e_4	e_5	e_6	e_7	e_8	r	$\|\|\boldsymbol{\mu}\|\|_\infty$	$\|\|\boldsymbol{\sigma}\|\|_\infty$	$\mathscr{H}_2$	$\|\|\boldsymbol{P}\|\|_\infty$	$\bar{t}_e$
Init. Model	μ_k	0.133	−0.248	0.539	−0.291	−0.176	0.467	0.514	−0.133	0.9576	0.539	0.055	0.367	3.601×10^{-6}	118.460s
	σ_k^2	0.051	0.038	0.045	0.036	0.045	0.046	0.055	0.051						
	$\widetilde{p}_k$	2.473×10^{-5}	1.192×10^{-6}	0.129	1.284×10^{-6}	4.909×10^{-6}	0.035	0.836	2.473×10^{-5}						
	r_k	0	0	0.179	0	0	0.070	0.751	0						
Max. r	μ_k	-0.042	0.231	0.251	−0.482	−0.087	0.569	0.184	−0.458	0.9819	0.569	0.054	0.365	2.464×10^{-6}	151.223s
	σ_k^2	0.051	0.037	0.042	0.036	0.045	0.048	0.051	0.054						
	$\widetilde{p}_k$	1.829×10^{-6}	5.459×10^{-7}	2.103×10^{-5}	0.002	4.173×10^{-7}	0.738	1.359×10^{-4}	0.260						
	r_k	0	0	0	0.007	0	0.717	0	0.276						
Min. $\|\|\boldsymbol{\mu}\|\|_\infty$	μ_k	0.164	−0.160	0.484	−0.324	−0.160	0.484	0.484	−0.160	0.9623	0.484	0.055	0.366	1.722×10^{-6}	203.074s
	σ_k^2	0.051	0.037	0.044	0.035	0.045	0.047	0.055	0.051						
	$\widetilde{p}_k$	1.255×10^{-4}	6.565×10^{-8}	0.055	8.819×10^{-6}	6.133×10^{-6}	0.118	0.827	1.102×10^{-4}						
	r_k	0	0	0.096	0	0.001	0.157	0.745	0.001						
Min $\|\|\boldsymbol{\sigma}\|\|_\infty$	μ_k	0.015	0.015	0.378	−0.393	−0.128	0.521	0.318	−0.318	0.9778	0.521	0.052	0.362	6.740×10^{-7}	449.385s
	σ_k^2	0.051	0.037	0.043	0.036	0.045	0.047	0.052	0.052						
	$\widetilde{p}_k$	4.301×10^{-6}	4.628×10^{-10}	0.006	3.104×10^{-4}	6.512×10^{-6}	0.937	0.029	0.028						
	r_k	0	0	0.009	0.001	0	0.858	0.065	0.067						
Min. $\mathscr{H}_2$	μ_k	0.001	0.003	0.386	−0.388	−0.130	0.518	0.317	−0.319	0.9777	0.518	0.052	0.362	6.289×10^{-7}	469.604s
	σ_k^2	0.051	0.037	0.043	0.036	0.045	0.047	0.052	0.052						
	$\widetilde{p}_k$	4.118×10^{-6}	3.287×10^{-10}	0.008	2.781×10^{-4}	7.420×10^{-6}	0.931	0.030	0.031						
	r_k	0	0	0.025	0	0	0.872	0.053	0.050						
Min. $\|\|\boldsymbol{P}\|\|_\infty$	μ_k	−0.125	−0.193	0.505	−0.312	−0.166	0.478	0.352	−0.284	0.9720	0.505	0.053	0.364	2.052×10^{-7}	550.514s
	σ_k^2	0.051	0.037	0.044	0.035	0.045	0.047	0.053	0.052						
	$\widetilde{p}_k$	1.528×10^{-4}	1.074×10^{-6}	0.433	2.441×10^{-5}	3.255×10^{-5}	0.433	0.116	0.017						
	r_k	0	0	0.418	0.001	0	0.426	0.127	0.028						

In the proposed optimization framework, because both the synchronous state that determined in a deterministic system and the fluctuations of the phase differences in a stochastic system are considered, synchronization stability can be effectively enhanced. In addition, it is demonstrated in Table V again that the most vulnerable edge can be effectively identified by the probability of the phase difference hitting the boundary of the secure domain.

Example 6.2. *Consider the network in Fig. 5 with 40 nodes and 47 edges, which is generated randomly with the connecting probability between each pair of nodes being 0.06. There are 20 gray nodes that are selected randomly and indexed by even numbers. We set* $T = 10^5$, $\mathrm{dt} = 10^{-3}$, $N = 10^5$, *and* $b_i = 0.95$ *for all nodes. We formulate an initial model, in which we set* $\omega_i = -3$ *for gray nodes and* $\omega_i = 3$ *for other nodes and* $l_{ij} = 10$ *for all the edges. In optimization problems for the design of the coupling strength, we set* $\omega_i = -3$ *for gray nodes and* $\omega_i = 3$ *for other nodes,* $W = 470$ *and* $\underline{l}_{ij} = 1$, $\bar{l}_{ij} = 20$ *for all the edges. In the optimization problems for the design of the natural frequency,*

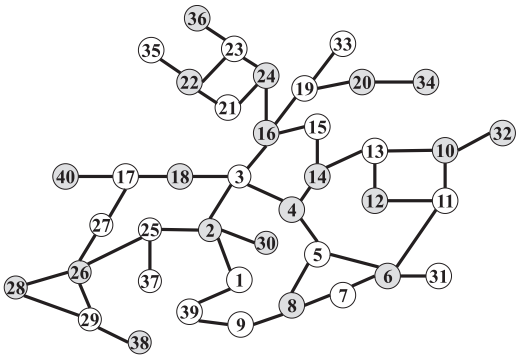

FIG. 5. A network with 40 nodes and 47 edges.

TABLE V. The most vulnerable edges identified by four metrics in the initial model and in the solutions to five optimization problems with respect to the design of the natural frequency for the network in Fig. 1.

	by u_k	by σ_k	by p_k	by r_k
Init. model	e_3	e_7	e_7	e_7
Max. r	e_6	e_8	e_6	e_6
Min. $\|\|\boldsymbol{\mu}\|\|_\infty$	e_7	e_7	e_7	e_7
Min. $\|\|\boldsymbol{\sigma}\|\|_\infty$	e_6	e_7	e_6	e_6
Min. $\mathscr{H}_2$	e_6	e_8	e_6	e_6
Min. $\|\|\boldsymbol{P}\|\|_\infty$	e_3	e_7	e_3	e_3

TABLE VI. The mean first hitting time $\bar{t}_e$ and values of objective functions in the initial model and in the solutions to five optimization problems with respect to the design of the coupling strength for the network in Fig. 5.

	r	$\|\|\boldsymbol{\mu}\|\|_\infty$	$\|\|\boldsymbol{\sigma}\|\|_\infty$	$\mathscr{H}_2$	$\|\|\boldsymbol{P}\|\|_\infty$	$\bar{t}_e$
Init. model	0.9148	0.644	0.056	1.824	4.723×10^{-5}	84.572s
Max. r	0.9685	0.338	0.178	2.683	1.989×10^{-4}	62.164s
Min. $\|\|\boldsymbol{\mu}\|\|_\infty$	0.9361	0.330	0.059	2.188	1.679×10^{-4}	65.439s
Min. $\|\|\boldsymbol{\sigma}\|\|_\infty$	0.9259	0.489	0.039	1.811	1.826×10^{-8}	2022.807s
Min. $\mathscr{H}_2$	0.9276	0.491	0.041	1.802	3.601×10^{-8}	1738.061s
Min. $\|\|\boldsymbol{P}\|\|_\infty$	0.9238	0.450	0.054	1.824	1.372×10^{-9}	4021.587s

TABLE VII. The mean first hitting time $\bar{t}_e$ and the values of the objective functions in the initial model and in the solutions of the 5 optimization problems with respect to the design of the natural frequency for the network in Fig. 5.

	r	$\|\|\boldsymbol{\mu}\|\|_\infty$	$\|\|\boldsymbol{\sigma}\|\|_\infty$	$\mathscr{H}_2$	$\|\|\boldsymbol{P}\|\|_\infty$	$\bar{t}_e$
Init. Model	0.9148	0.644	0.056	1.824	4.723×10^{-5}	84.572*s*
Max. r	0.9735	0.653	0.056	1.793	2.435×10^{-5}	130.249*s*
Min. $\|\|\boldsymbol{\mu}\|\|_\infty$	0.9329	0.536	0.056	1.795	1.364×10^{-5}	163.661*s*
Min. $\|\|\boldsymbol{\sigma}\|\|_\infty$	0.9445	0.643	0.051	1.784	5.969×10^{-6}	287.234*s*
Min. $\mathscr{H}_2$	0.9446	0.643	0.051	1.782	5.820×10^{-6}	294.689*s*
Min. $\|\|\boldsymbol{P}\|\|_\infty$	0.9412	0.640	0.053	1.795	1.543×10^{-6}	493.585*s*

we set $\underline{\omega}_i = -3$ *and* $\overline{\omega}_i = -3$ *for the grey nodes and* $\underline{\omega}_i = 0$ *and* $\overline{\omega}_i = 14$ *for the other nodes and* $l_{ij} = 10$ *for all the edges.*

For the design of the coupling strength and the natural frequency, the values of the objective functions of five optimization problems are shown in Tables VI and VII, respectively. As in the results of the network in Example 6.1, by maximizing the order parameter r and the phase cohesiveness measured by $\|\mu\|_\infty$ for the design of the coupling strength, the mean first hitting time decreases from about 85 to about 62 s and to about 65 s, respectively. This indicates again that a larger order parameter or a higher level phase cohesiveness does not mean that the system is more robust against disturbances. However, using the proposed optimization framework, the mean first hitting time increases from about 85 to about 4021 s, which is much more effective than minimizing the largest variance of phase differences and the $\mathscr{H}_2$ norm. In addition, in the design of the natural frequency, the mean first hitting time increases from about 85 to about 494 s by the proposed optimization framework. These findings demonstrate that the proposed optimization framework can effectively increase synchronization stability of the complex system.

VII. CONCLUSION

In this paper, based on the theory of the invariant probability distribution of stochastic Gaussian processes, we have proposed a new metric for synchronization stability of complex networks, that is the probability of the state being absent from a secure domain. By this metric, the most vulnerable edges that may lead to desynchronization can be precisely identified. Using this metric as objective functions of optimization problems, either the natural frequencies or the coupling strength can be assigned to improve synchronization stability. It is demonstrated in the case studies that by optimizing this metric, the mean first hitting time when the state of the system under stochastic disturbances hits the boundary of the secure domain can be effectively increased. In contrast, optimization of either the order parameter or the phase cohesiveness defined for a deterministic model may dramatically decrease the mean first hitting time and further decreases synchronization stability. This indicates that it is more practical to study synchronization stability with the consideration of the strength of the disturbances as in the stochastic process.

However, compared with the traditional methods for the synchronization stability analysis in the deterministic model, the strength of disturbances has to be identified in the model of the stochastic processes, and a matrix spectral decomposition is needed to compute the invariant probability distribution of the phase difference. In order to apply the proposed optimization framework to improve the synchronization stability of a large-scale system in practice, efficient algorithms for spectral decomposition and for optimization problems are important, which are the focus of the future research.

ACKNOWLEDGMENTS

This work was financially supported by the National Natural Science Foundation with Grant No. 62103235 and the Shandong Provincial Natural Science Foundation, China, with Grant No. ZR2020QF118.

AUTHOR DECLARATIONS

Conflict of Interest

The authors have no conflicts to disclose.

Author Contributions

Xian Wu: Formal analysis (equal); Investigation (equal); Methodology (equal); Writing – review & editing (equal). **Kaihua Xi:** Conceptualization (equal); Formal analysis (equal); Investigation (equal); Methodology (equal); Project administration (equal); Supervision (equal); Writing – review & editing (lead). **Aijie Cheng:** Project administration (equal); Supervision (equal). **Hai Xiang Lin:** Supervision (equal); Writing – review & editing (equal). **Jan H. van Schuppen:** Conceptualization (equal); Supervision (equal); Writing – review & editing (equal).

DATA AVAILABILITY

The data that support the findings of this study are available within the article.

APPENDIX A: THE OPTIMIZATION PROBLEMS FOR THE CASE STUDY

The order parameter of the couple phase oscillators is defined as

$$re^{\mathrm{i}\phi} = \frac{1}{n}\sum_{j=1}^{n} e^{\mathrm{i}\varphi_j},$$

where $\mathrm{i}^2 = -1$ and φ_j is the phase at node j and $re^{\mathrm{i}\phi}$ is the phase" centroid on the complex unit circle with the magnitude r ranging from 0 to 1.[23] In the case study, the order parameter is maximized by solving the following optimization problem:[9]

$$\begin{aligned} &\min_{l_{ij}\in\mathbb{R},(i,j)\in\mathcal{E}} \; r = 1 - ||\boldsymbol{\varphi}||^2/n, \\ &\text{s.t } (28b), (28c), \\ &\boldsymbol{\varphi}^* = \boldsymbol{L}^\dagger \boldsymbol{\omega}, \end{aligned} \tag{A1}$$

where the matrix $\boldsymbol{L}^{\dagger}$ is defined in (21), and the one for the design of the natural frequency is

$$\begin{aligned} &\min_{\omega_i\in\mathbb{R},i\in\mathcal{V}} r = 1-||\boldsymbol{\varphi}^*||^2/n,\\ &\text{s.t (29c), (29d),}\\ &\boldsymbol{\varphi}^* = \boldsymbol{L}^{\dagger}\boldsymbol{\omega}. \end{aligned} \tag{A2}$$

The optimization problem for the design of the coupling strength with the objective of increasing the phase cohesiveness is

$$\begin{aligned} &\min_{l_{ij}\in\mathbb{R},(i,j)\in\mathcal{E}} ||\boldsymbol{y}^*||_\infty,\\ &\text{s.t (2), (7), (28b), (28c),} \end{aligned} \tag{A3}$$

and the one for the design of the natural frequency with this objective is

$$\begin{aligned} &\min_{\omega_i\in\mathbb{R},i\in\mathcal{V}} ||\boldsymbol{y}^*||_\infty,\\ &\text{s.t (2), (7), (29c), (29d).} \end{aligned} \tag{A4}$$

In the section of case study, the optimization problem for designing the coupling strength with the objective of minimizing the $\mathscr{H}_2$ norm follows:

$$\begin{aligned} &\min_{l_{ij}\in\mathbb{R},(i,j)\in\mathcal{E}} \mathrm{tr}(\boldsymbol{Q}_{\tilde{y}}),\\ &\text{s.t (2), (11), (15), (16), (28b), (28c),} \end{aligned} \tag{A5}$$

and the one to redistribute the natural frequency with this objective is

$$\begin{aligned} &\min_{\omega_i\in\mathbb{R},i\in\mathcal{V}} \mathrm{tr}(\boldsymbol{Q}_{\tilde{y}}),\\ &\text{s.t (2), (11), (15), (16), (29c), (29d).} \end{aligned} \tag{A6}$$

If the maximum of the variances of the phase differences in the edges is minimized, the objective function is replaced by $||\boldsymbol{\sigma}||_\infty$ in the above two optimization problems.

APPENDIX B: THE INVARIANT PROBABILITY DISTRIBUTION AND $\mathscr{H}_2$ NORM

Consider a linear time-invariant system,

$$\dot{\boldsymbol{x}} = \boldsymbol{A}\boldsymbol{x} + \boldsymbol{B}\boldsymbol{w}, \tag{B1a}$$

$$\boldsymbol{y} = \boldsymbol{C}\boldsymbol{x}, \tag{B1b}$$

where $\boldsymbol{x}\in\mathbb{R}^{n_x}$, $\boldsymbol{A}\in\mathbb{R}^{n_x\times n_x}$ is Hurwitz, $\boldsymbol{B}\in\mathbb{R}^{n_x\times n_w}$, $\boldsymbol{C}\in\mathbb{R}^{n_y\times n_x}$, the input is denoted by $\boldsymbol{w}\in\mathbb{R}^{n_w}$ and the output of the system is denoted by $\boldsymbol{y}\in\mathbb{R}^{n_y}$. The squared $\mathscr{H}_2$ norm of the transfer matrix $\boldsymbol{G}$ of mapping $(\boldsymbol{A},\boldsymbol{B},\boldsymbol{C})$ from the input $\boldsymbol{w}$ to the output $\boldsymbol{y}$ is defined as

$$||\boldsymbol{G}||_2^2 = \mathrm{tr}(\boldsymbol{B}^T\boldsymbol{Q}_o\boldsymbol{B}) = \mathrm{tr}(\boldsymbol{C}\boldsymbol{Q}_c\boldsymbol{C}^T), \tag{B2a}$$

$$\boldsymbol{Q}_o\boldsymbol{A} + \boldsymbol{A}^T\boldsymbol{Q}_o + \boldsymbol{C}^T\boldsymbol{C} = \boldsymbol{0}, \tag{B2b}$$

$$\boldsymbol{A}\boldsymbol{Q}_c + \boldsymbol{Q}_c\boldsymbol{A}^T + \boldsymbol{B}\boldsymbol{B}^T = \boldsymbol{0}, \tag{B2c}$$

where $\mathrm{tr}(\cdot)$ denotes the trace of a matrix and $\boldsymbol{Q}_o, \boldsymbol{Q}_c\in\mathbb{R}^{n_x\times n_x}$ are the *observability Grammian* of $(\boldsymbol{C},\boldsymbol{A})$ and *controllability Grammian* of $(\boldsymbol{A},\boldsymbol{B})$, respectively.[24,25] When the input $\boldsymbol{w}$ is modelled by Gaussian white noise, the distribution of the state $\boldsymbol{x}$ and the output $\boldsymbol{y}$ are also Gaussian. Denote then for all $t\in T$, $\boldsymbol{x}(t)\in G(\boldsymbol{m}_x(t),\ \boldsymbol{Q}_x(t))$ with $\boldsymbol{Q}_x(t)\in\mathbb{R}^{n_x\times n_x}$ and $\boldsymbol{y}(t)\in G(\boldsymbol{m}_y(t),\ \boldsymbol{Q}_y(t))$ with $\boldsymbol{Q}_y(t)\in\mathbb{R}^{n_y\times n_y}$. Because the matrix $\boldsymbol{A}$ is Hurwitz, there exists an invariant probability distribution of this linear stochastic system with the representation and properties,

$$\boldsymbol{0} = \lim_{t\to\infty}\mathbf{m}_x(t),\ \boldsymbol{0} = \lim_{t\to\infty}\boldsymbol{m}_y(t),$$

$$\boldsymbol{Q}_x = \lim_{t\to\infty}\boldsymbol{Q}_x(t), \boldsymbol{Q}_y = \lim_{t\to\infty}\boldsymbol{Q}_y(t),$$

where the variance matrices are

$$\boldsymbol{Q}_x = \int_0^{+\infty}\exp(\boldsymbol{A}t)\boldsymbol{B}\boldsymbol{B}^{\top}\exp(\boldsymbol{A}^{\top}t)\mathrm{d}t,\ \boldsymbol{Q}_y = \boldsymbol{C}\boldsymbol{Q}_x\boldsymbol{C}^{\top}.$$

Here, $\boldsymbol{Q}_x$ is the unique solution of the Lyapunov matrix function (B2c).

REFERENCES

[1] D. M. Abrams and S. H. Strogatz, "Chimera states for coupled oscillators," Phys. Rev. Lett. **93**, 174102 (2004).
[2] L. Glass and M. C. Mackey, *From Clocks to Chaos: The Rhythms of Life* (Princeton University Press, Princeton, NJ, 1988).
[3] C. Ma and J. Zhang, "Necessary and sufficient conditions for consensusability of linear multi-agent systems," IEEE Trans. Autom. Control **55**, 1263–1268 (2010).
[4] T. Yang, X. Yi, J. Wu, Y. Yuan, D. Wu, Z. Meng, Y. Hong, H. Wang, Z. Lin, and K. H. Johansson, "A survey of distributed optimization," Annu. Rev. Control **47**, 278–305 (2019).
[5] K. Xi, J. L. A. Dubbeldam, and H. X. Lin, "Synchronization of cyclic power grids: Equilibria and stability of the synchronous state," Chaos **27**, 013109 (2017).
[6] A. E. Motter, S. A. Myers, M. Anghel, and T. Nishikawa, "Spontaneous synchrony in power-grid networks," Nat. Phys. **9**, 191–197 (2013).
[7] F. Dörfler and F. Bullo, "Synchronization in complex networks of phase oscillators: A survey," Automatica **50**, 1539–1564 (2014).
[8] M. Fazlyab, F. Dörfler, and V. M. Preciado, "Optimal network design for synchronization of coupled oscillators," Automatica **84**, 181–189 (2017).
[9] P. S. Skardal, D. Taylor, and J. Sun, "Optimal synchronization of complex networks," Phys. Rev. Lett. **113**, 144101 (2014).
[10] L. M. Pecora and T. L. Carroll, "Master stability functions for synchronized coupled systems," Phys. Rev. Lett. **80**, 2109–2112 (1998).
[11] P. J. Menck, J. Heitzig, N. Marwan, and J. Kurths, "How basin stability complements the linear-stability paradigm," Nat. Phys. **9**, 89–92 (2013).
[12] R. Delabays, M. Tyloo, and P. Jacquod, "The size of the sync basin revisited," Chaos **27**, 103109 (2017).
[13] B. K. Poolla, S. Bolognani, and F. Dörfler, "Optimal placement of virtual inertia in power grids," IEEE Trans. Autom. Control **62**, 6209–6220 (2017).
[14] E. Tegling, B. Bamieh, and D. F. Gayme, "The price of synchrony: Evaluating the resistive losses in synchronizing power networks," IEEE Trans. Control Netw. Syst. **2**, 254–266 (2015).
[15] M. Tyloo, T. Coletta, and P. Jacquod, "Robustness of synchrony in complex networks and generalized Kirchhoff indices," Phys. Rev. Lett. **120**, 084101 (2018).
[16] K. Xi, Z. Wang, A. Cheng, H. X. Lin, J. H. van Schuppen, and C. Zhang, "Synchronization of complex network systems with stochastic disturbances," arXiv:2201.07213 (2022).
[17] M. M. Klosek-Dygas, B. J. Matkowsky, and Z. Schuss, "Stochastic stability of nonlinear oscillators," SIAM J. Appl. Math. **48**, 1115–1127 (1988).
[18] M.-L. T. Lee and G. A. Whitmore, "Threshold regression for survival analysis: Modeling event times by a stochastic process reaching a boundary," Stat. Sci. **21**, 501–513 (2006).
[19] A. Jadbabaie, N. Motee, and M. Barahona, "On the stability of the Kuramoto model of coupled nonlinear oscillators," in *Proceedings of the 2004 American Control Conference* (IEEE, 2004), Vol. 5, pp. 4296–4301.

[20]F. Dörfler and F. Bullo, "On the critical coupling for Kuramoto oscillators," SIAM J. Appl. Dyn. Syst. **10**, 1070–1099 (2011).
[21]S. Albeverio and V. N. Kolokoltsov, "The rate of escape for some gaussian processes and the scattering theory for their small perturbations," Stoch. Process Appl. **67**, 139–159 (1997).
[22]L. M. Ricciardi and S. Sato, "First-passage-time density and moments of the Ornstein-Uhlenbeck process," J. Appl. Probab. **25**, 43–57 (1988).
[23]Y. Kuramoto, *Chemical Oscillations, Waves and Turbulence* (Springer, New York, 1984).
[24]J. C. Doyle, K. Glover, P. P. Khargonekar, and B. A. Francis, "State-space solutions to standard H2 and H infinty control problems," IEEE Trans. Autom. Control **34**, 831–847 (1989).
[25]R. Toscano, *Structured Controllers for Uncertain Systems* (Springer-verlag, London, 2013).